Functional Compensation Dominates Plant Rhizosphere Microbiota Assembly

Yi Ren
Nanjing Agricultural University
Weibing Xun (xunwb@njau.edu.cn)
Nanjing Agricultural University College of Resources and Environmental Sciences
https://orcid.org/0000-0003-0068-8514
He Yan
Nanjing Agricultural University
Aiyuan Ma
Nanjing Agricultural University
Wu Xiong
Nanjing Agricultural University
Qirong Shen
Nanjing Agricultural University
Ruifu Zhang
Nanjing Agricultural University

Research

Keywords: rhizospheremicrobiota, functional assembly, transplant, soil fertility, functional characteristics

Posted Date: May 5th, 2020

DOI: https://doi.org/10.21203/rs.3.rs-25976/v1

Abstract

Background: Rhizospheremicrobiota plays a key role in plant-soil feedbacks, yet the intrinsic principles governing rhizospheremicrobiota assembly remain unclear. To understand the principles, we studied taxonomical and functional characteristics of re-assembled maize rhizospheremicrobiota during transplanting between soils. The composition of rhizospheremicrobiota were measured by High-throughput amplicon-based IlluminaMiSeq sequencing of 16S ribosomal RNA (rRNA) gene V4-region. The rhizosphere functional profiles were assessed using 16S rRNA data through PICRUSt (Phylogenetic Investigation of Communities by Reconstruction of Unobserved State) software.

Results: The re-assembled rhizospheremicrobiota was recruited from both soil and endosphere communities. Soil nutrient availability dominatedmicrobiota assembly and functional profile in rhizosphere. The most important rhizospheric functions were stress tolerance, while the related taxa were in low abundance and derived primarily from bulk soil. Nutrient excessive soil marginalized rhizosphere nutrient cycling functions, while nutrient deficient soil sacrificed stress tolerance functions and enhanced compensatory colonization of nutrient cycling related endophytes in rhizosphere.

Conclusions: Our results demonstrate soil condition mediates rhizospheremicrobiota assembly to satisfy plant required functions. This assembly principle is helpful for manipulating plant root microbiota to improve agricultural sustainability.

Background

Rhizosphere microbes growing in association with plant roots are crucial for plant productivity because of their irreplaceable roles in soil nutrients cycling [1], abiotic stress toleration [2] and soil-borne pathogen suppression [3]. Previous researches provide comprehensive evidences that rhizosphere microbiota is largely shaped by surrounding environment, including geographical location, soil nutrient content and availability [4, 5], plant exuded carbon and other metabolites [6], plant genotype [7] and developmental stage [8]. Rhizosphere microbiota vary greatly in spatio-temporal distributions [9] and preserve a dynamic equilibrium state integrates both ‘outside-in’ transmission from surrounding soil [10] and ‘inside-out’ transmission through released endophytes [11]. These complicated features make exploration of general principles governing rhizosphere microbiota assembly more challenging.

A key to rhizosphere microbiota assembly is suggested to be functional traits, potentially because the functional profiles are less affected by microbiota variations [12]. Consequently, the focus should not only on the microbial taxa recruited by the host plant, but also on the functions for plant fitness, especially by promoting nutrient cycling and abiotic/biotic stress tolerance, and the priority of these functions under different soil conditions. Heritable taxa in maize rhizosphere have been identified by large-scale investigation [9, 13], in which some specific members can benefit plant by providing pathogen suppression [14] and supplying available nutrients [15]. The rhizosphere microbiota assembly of an annual grass is dependent on plant exudation and microbial substrate uptake traits, in which chemical

components succession in rhizosphere make the functional members often in dynamic succession [6]. However, the general principles underpinning rhizosphere microbiome assembly is poorly understood. Thus, a current research challenge is to understand what principles that dominate the compositional and functional assembly of rhizosphere microbiota.

Here, we present a study by transplanting the maize seedlings between distinct soils and addressing compositional and functional rhizosphere microbiota successions under various soil conditions. Three types of soil are collected for this research, the black, paddy and red soils are classified as Calcaric Chernozems, Orthic Acrisol and Ferralic Cambisol respectively, according to FAO/Unesco System of Soil Classification (Additional file: Table S1). We hypothesize that plants recruit different rhizosphere microbiotas to satisfy required functions for their fitness in different soil conditions.

Methods

Soil collection and characteristic analyses

Three types of soil were collected from different parts of China in August, 2016. Black soil, paddy soil and red soil samples were collected from Qiqihaer (123°62'E, 47°64'N) in Heilongjiang Province of Northeast China, Taizhou (120°20' E, 32°44' N) in Jiangsu Province of East China and Yingtan (116°94'E, 28°21'N) in Jiangxi Province of South China, respectively. The black, paddy and red soils are classified as Calcaric Chernozems, Orthic Acrisol and Ferralic Cambisol respectively, according to FAO/Unesco System of Soil Classification. Samples were obtained from the upper 20 cm of soil perennially covered by weeds. All samples were sieved with a 2 mm sieve removing visible plant tissues and stones, after which they were temporarily preserved in a portable storage box and transported to the lab immediately. Subsamples for measuring physiochemical properties were air-dried. Subsamples for pot experiment were stored at room temperature (25 ^{o}C) until use.

The following physio-chemical properties were measured to assess soil characteristics: (i) the soil pH was determined using a PHS − 3C mv/pH detector (Shanghai, China) at a soil-to-water ratio of 1:5; (ii) the available K (AK) in the soil was extracted with ammonium acetate and determined using flame photometry; (iii) the available P (AP) in the soil was extracted with sodium bicarbonate and then determined using the molybdenum blue method; (iv) the total N (TN) was determined via Kjeldahl digestion; (v) the total P (TP) and total K (TK) were extracted with HF–HClO4 and determined via molybdenum-blue colorimetry and flame photometry, respectively; (vi) the soil organic matter (OM) was determined using the potassium dichromate volumetric method; (vii) the cation exchange capacity (CEC) was measured using the ammonium acetate exchange method; (viii) the specific conductance (SC) was determined using 5:1 (liquid/soil) leach liquor and conductometer for calculation.

Experimental Setup

The maize used in this study is hybridized from male parent plant H9822 and female parent plant H9801, which is widely cultivated in coastal areas of China. Firstly, the seeds were soaked in sterilized water (25 ^{o}C) for 6 hours and then in 70% ethanol for 1 min. After that, the seeds were washed by sterile distilled water for three times. Then, the seeds were soaked in 2% Sodium hypochlorite solution for 10 min and washed by sterile distilled water for another three times. After surface sterilization, all seeds were spread on a sterilized plate for germinating in an artificial climate chamber under the condition of 16 h light at 22 ^{o}C and 8 h dark at 18 ^{o}C for 4 days.

The 4 days old seedlings were transplanted from plate to sterile (autoclaved) cylindrical pots (12 cm in diameter and 15 cm in height) with 1,000 g one type of fresh soil inside, with 2 seedlings per pot. Some pots were designated 'bulk soil' without plant. Including bulk soil controls, all pots were spatially randomized and placed in growth chambers providing 16 h light at 22 ^{o}C and 8 h dark at 18 ^{o}C and were watered during cultivation with sterile distilled water as an accessible imitation for rain water but without other chemical additives.

For time-series sampling, we established 20 replicated pots and 4 pots were randomly chosen for sampling at each sampling time (Fig. 1a and Additional file: Table S2). The rhizosphere and root samples were collected at successive intervals (0, 6, 9, 12, 16, and 20 days) with day 0 as the equivalent to soil and seed.

For transplanting experiment, after 8 days cultivation, a proportion of pots with the same soil were randomly chosen for sampling and the rest were used for transplanting (Fig. 1d and Additional file: Table S3). For transplantation, loose soil was manually removed from the roots without any damage on roots, and the roots were gently flushed with running water to wash soil away as possible. Then, roots were washed in sterile Phosphate Buffer (PBS-S, per litre: 6.33 g of $NaH_2PO_4 \cdot H_2O$, 16.5 g of $Na_2HPO_4 \cdot 7H_2O$, 200 µL Silwet L-77) on shaking tables (80 Hz) for 30 min, followed by sterile distilled water washing for 3 times. After that, the plants were sonicated for 3 min with 30 s pulses at 60 Hz and 30 s breaks (power 220 V, ultrasonic cleaner KH5200DB, Kunshan ultrasonic instrument Co., Ltd., Kunshan, China) in order to wipe out tiny soil aggregates and root surface microorganisms [4, 8]. The washed plants were then transplanted to distinct soils and cultivated for another 8 days (Fig. 1d). Sampling was performed after cultivation (Additional file: Table S3).

Sampling

Bulk soil samples were collected from 1 cm below the surface in the control pots. Soil samples were placed into 2 mL clean and sterile centrifuge tubes. The samples were flash-frozen using liquid nitrogen and stored in -80 ^{o}C until DNA extraction.

For rhizosphere sampling, the aboveground plant organs were aseptically removed, loose soil (> 1 mm, not the rhizosphere soil) was manually removed with sterile rubber gloves (sprinkled with 70% EtOH) leaving approximately 1 mm soil on roots. Roots were placed in a clean and sterile 50 mL tube containing

30 mL PBS-S solution and vortex at maximum speed for 15 s (Vortex-Gene 2, Scientific Industries, USA). Next, a new clean and sterile 50 mL tube with 100 μm nylon mesh cell strainer was used to filter the plant organism and large sediment from rhizosphere soil [4], and repeat this step with 10 mL PBS-S solution to obtain a more complete rhizosphere sample. The turbid filtrate was then centrifuged for 15 min at 3,500 g to form a pellet with nice sediment and microbes. We discarded the supernatant and added 1 mL PBS-S solution to resuspend by votex. Then the suspension was transported to a sterile 2 mL microfuge tubes and centrifuged for 5 min at 10,000 g to form firmly pellets. A flash-frozen was conduct using liquid nitrogen after discarding the supernatant and stored at -80 ^{O}C until DNA extraction.

For endosphere sampling, the roots after cell strainer filtering were transferred to a new sterile 50 mL tube with 30 mL PBS-S solution and sonicated at 60 Hz for 3 min (3 cycle: 30 s sonication and 30 s break) to remove the surface microbes. After sonication, the roots were transferred to a 2 mL centrifuge tube with sterile tweezers and flash-frozen using liquid nitrogen. The samples were stored in -80 ^{O}C until DNA extraction.

Dna Extraction And 16s Rrna Gene Amplicon Sequencing

The liquid nitrogen frozen root samples were preprocessed by bead beating using a plant grinder (DHS TL2020, 0401261, DHS Technology Co., Ltd., Beijing, China) for 5 min at 1,800 rpm (5 cycle: 30 s vibrate and 30 s break). Then, total DNA of all bulk soil, rhizosphere soil and root samples were extracted from 0.25 g of sample using the QIAGEN DNeasy PowerSoil Kit (Ref: 12888-100, Germany). To minimize DNA extraction bias, three successive DNA extractions of each sample were pooled before performing polymerase chain reaction (PCR). A NanoDrop ND-2000 spectrophotometer (NanoDrop, ND2000, Thermo Scientific, 111 Wilmington, DE, USA) was used to assess DNA quality according to the 260/280-nm and 260/230-nm absorbance ratios.

Amplification of the V4 hypervariable region of the bacterial 16S rRNA gene was performed to assess the bacterial community using the primers 515F: 5’-GTGYCAGCMGCCGCGGTAA-3’ and 806R: 5’-GGACTACNVGGGTWTCTAA-3’. PCR amplifications were combined in equimolar ratios and sequenced on an Illumina MiSeq instrument (300-bp pairedend reads). The sequencing data were processed using the UPARSE pipeline (http://drive5.com/usearch/manual/uparse_pipeline.html) [26]. Raw sequences were first trimmed at length of 220 bp using command “fastx_truncate” to discard shorter sequences, the paired-end sequences were assembled using the command “fastq_mergepairs”. Then, high-quality sequences were reaped by “fastq_filter” command and dereplicated by “fastx_uniques” command. Singleton and chimeric sequences were removed after dereplication. The remaining sequences were clustered into operational taxonomic units (OTUs) at 97% similarity and taxonomic assignment was performed using the Greengenes 16S rRNA database (released on 2013/5). For each treatment, we made zero if an OTU has less than 3/4 (time-series samples) or 4/6 (transplanting samples) detected values among duplicates. At last, a rarefied OTU table at 5000 reads per sample was created using the USEARCH command “otutab_norm”.

Statistical analysis

Relative abundance of one phylogenetic group was defined as the number of sequences affiliated with that group divided by the total number of sequences per sample. The Shannon diversity index (α-diversity) calculation, Bray-Curtis dissimilarity-based PCA analysis and permutational multivariate analysis of variance (PERMANOVA) were performed based on the rarefied OTU table using the vegan R package (v.2.5-2) (https://cran.r-project.org/package=vegan). Tukey's HSD test was used to calculate the significance between two samples. All statistical analyses were performed using R software (v.3.5.1).

The phylogenetic tree of the top 100 OTUs in relative abundance was constructed by FastTree (v.2.1.3) [27] and visualized by iTol (https://itol.embl.de/). The ternary plots were conducted using edgeR R package (v.3.22.3) (http://www.bioconductor.org/packages/release/bioc/html/edgeR.html) and visualized by ggplot2 R package (v.2.2.1) (https://cran.r-project.org/package=ggplot2). The Venn diagrams were calculated and visualized using the online tool Venny (https://bioinfogp.cnb.csic.es/tools/venny/). Sankey plots reveal the OTU flows as well as the composition among different samples [28] were constructed using the custom scripts based on D3.js (v.5.14.2) (d3js.org).

Network analysis was used to represent the co-occurrence pattern in a complex community. We conduct co-occurrence network analysis in different rhizosphere samples based on rarefied OTU table. A valid co-occurrence was considered as a statistically significant correlation between OTUs if the spearman's correlation coefficient $r > 0.75$ and P-value < 0.01. The P-values were adjusted by multiple testing correction using the Benjamini-Hochberg's FDR (false discovery rate) method [29] to reduce the chance of obtaining false-positive results.

The network analyses were performed using the psych R package (v.1.8.12) (https://cran.r-project.org/package=psych). Co-occurrence networks were visualized using Gephi software (v.0.9.2) [30]. We constructed bipartite network to feature the OTU sharing among samples [31] through the "Edge-weighted spring-embedded algorithm" method after trimming the OTU table at a 0.05% relative abundance threshold. The bipartite network was visualized using Cytoscape (v.3.6.1) [32].

The PICRUSt software [16] was applied to predict KEGG Ortholog (KO) functional profiles [33] of microbial communities using 16S rRNA gene sequences (Additional file: Figure S1). The overall functional characteristics ("Total Function") displayed in ternary plot and PCA plots were analyzed using the KOs count table supplied by PICRUSt software. For segmented function analysis, firstly, the importance of OTU in each network was defined using the degree of each OTU in co-occurrence network. Secondly, the OTUs were segmented into a series of functional OTU clusters from the most important OTU to the least important OTU. Thirdly, "Segmented Predicted Function" of every OTU cluster was predicted using PICRUSt software, respectively. Meanwhile, a "Segmented Theoretical Function" of each OTU cluster was calculated using relative abundance ("OTU RA", the relative abundance of each segmented OTU cluster) adjusted overall community function (Eq. 1).

$$\text{Segmented Theoretical Function} = \text{Total Function} \times \text{OTU RA} \quad \text{(Eq. 1)}$$

Importantly, we summed the “Segmented Predicted Function” of all OTU clusters and found the results are exactly the same as the “Total Function”. To define the enriched or depleted functions of each OTU cluster, we calculated the “Segmented enriched or depleted function” using the “Segmented Predicted Function” and “Segmented Theoretical Function” (Eq. 2). The enriched or depleted functions were visualized in MATLAB (v.7.14.0.739).

$$\text{Segmented enriched(depleted)function} = \frac{|\text{Segmented Predicted Function} - \text{Segmented Theoretical Function}|}{\text{Segmented Theoretical Function}} \quad \text{(Eq. 2)}$$

Results

Before establishing transplant experiment, a time-series longitudinal dense sampling in pot trials was performed to identify an appropriate transplanting time point. We first collected the rhizosphere and root samples at successive intervals (0, 6, 9, 12, 16, and 20 days) (Fig. 1a), yielding 52 samples (Additional file: Table S2). Bacterial communities were measured by High-throughput amplicon-based Illumina MiSeq sequencing of 16S ribosomal RNA (rRNA) gene V4-region. Variance adjusted Weighted_UniFrac dissimilarity was performed to compare microbiota compositions. Compare to the root-associated microbiota on day 20, patterns of Weighted_UniFrac dissimilarity within rhizosphere (Fig. 1b) and endosphere (Fig. 1c) microbiotas were less varied after 12 days. Then, the 12 days old maize seedlings were transplanted from black soil to paddy and red soils, and also from paddy and red soils to black soil (Fig. 1d), which allowed us to infer the compositional and functional assembly of rhizosphere microbiota from heterologous soil and endosphere microbiotas. Consequently, we collected bulk soil, rhizosphere and endosphere samples on both day 12 and day 20, yielding 150 samples (Additional file: Table S3). The Illumina MiSeq sequencing (16S rRNA, V4-region) produced 2,465,250 sequences, averaging 16,435 reads per sample.

Re-assembled Rhizosphere Microbiotas Were Compositionally Divergent

Before transplanting, bacterial shannon diversity was the lowest in red soil (Additional file: Figure S2a). Plant recruitment decreased the diversity from soil to rhizosphere and then to endosphere. Actinobacteria was enriched while Acidobacteria was depleted by plant recruitment (Additional file: Figure S2b). Red soil contained many unique taxonomic groups due to distinct soil pH (32.85% of the variation) (Additional file: Figure S2c), whereas black and paddy soils shared large proportions of taxonomic groups, and compartment became main driving force of microbiotas (25.60% of the variation). Many Betaproteobacterial groups were abundant in red soil, while Gammaproteobacterial groups were

abundant in paddy and black soils (Fig. 2a). This distinguished soil and endosphere communities facilitated tracing species sources of re-assembled rhizosphere microbiota after transplanting.

After transplanting, the overall bacterial composition of bulk soils (Additional file: Figure S3a) and the trends of shannon diversity indices associated with soil type and compartment (Additional file: Figure S3b) did not change. The rhizosphere microbiotas tended to be similar after transplanted to black soil (ANOSIM R-value = 0.352, *P*-value = 0.047) (Additional file: Figures S3c to S3e), whereas were distinct among soils after transplanted to different soils (ANOSIM R-value = 0.644, *P*-value < 0.001) (Additional file: Figure S3f). Particularly, after transplanted from black soil to other soils, the Betaproteobacterial groups were enriched in R_BtoR (21.3% in proportion) and E_BtoR (35.7% in proportion), but were observed with low abundance in R_BtoP (8.7% in proportion), E_BtoP (4.6% in proportion), R_BtoB (6.0% in proportion) and E_BtoB (7.8% in proportion) (Fig. 2b). However, due to the introducing of endosphere microbiota originated from black soil, more shared bacteria were observed in rhizosphere (Fig. 2c). We found the Gammaproteobacterial groups were enriched in rhizosphere (49.7% in R_BtoB, 57.7% in R_BtoR, and 41.7% in R_BtoP) and endosphere microbiotas (45.2% in E_BtoB, 43.0% in E_BtoR, and 39.2% in E_BtoP) (Fig. 2b).

Re-assembled Rhizosphere Microbiotas Were Functionally Less Divergent

Above 16S rRNA gene survey revealed a clear differentiation among rhizosphere microbiota compositions after transplanting. To evaluate how these compositional changes alter rhizosphere functional profiles, we predicted community functions using 16S rRNA data through PICRUSt software [16]. We detected variations in predicted genes related to the “metabolism” functions in KEEG (Kyoto Encyclopedia of Genes and Genomes) pathway. Transplanting did not change the overall functions of bulk soils, but each soil had its preferential functions (Additional file: Figure S4a). Plant rhizosphere microbiota recruited from different environments shared greater function similarity than taxonomy (Fig. 3a). The rhizosphere functional profiles were distinct among soils before transplanting (ANOSIM R-value = 0.885, *P*-value = 0.002) and were similar after transplanted from black soil to other soils (ANOSIM R-value = 0.634, *P*-value = 0.006) (Figs. 3b and 3c), and were even more similar after transplanted from other soils to black soil (ANOSIM R-value = 0.284, *P*-value = 0.024) (Additional file: Figures S4b and S4c).

Soil fertility determined the dominant functional profiles of re-assembled rhizosphere microbiotas

To investigate functional characteristics of nutrient cycling and abiotic/biotic stress tolerance in rhizosphere after transplanting, we firstly constructed co-occurrence network between different OTUs (Additional file: Figure S5a) and defined keystone taxa (Additional file: Table S4). Then, we ranked OTUs according to node degree and segmented them into OTU clusters from the greatest (highest node degree)

to the lowest importance (lowest node degree). Next, we predicted functions of OTU clusters segmentally. The enriched or depleted functions (Additional file: Table S5) were evaluated by comparing predicted and theoretical functions (Additional file: Figure S1).

The functional profiles of rhizosphere microbiota showed different patterns among these soils (Fig. 4a and Additional file: Figure S5b). In black soil, the top 30% most important OTUs enriched the functions of “glycan biosynthesis and metabolism” and “biosynthesis of other secondary metabolites”, including “Flavonoid biosynthesis”, “Streptomycin biosynthesis” and “Glycosphingolipid biosynthesis”, which are generally involved in enhancing plant abiotic/biotic stress tolerance [17, 18]. The following intermediate important OTUs (between 30–60% importance) enriched functions related to nutrient cycling, including “nitrogen, phosphorus and sulfur metabolism”, “carbohydrate metabolism” and “xenobiotics biodegradation and metabolism”, etc. In paddy soil, excessive available nutrients (Additional file: Table S1) initiated a clear marginalization (the 50% least important OTUs) of nutrient cycling functions. However, in red soil, nutrient deficiency triggered increasing importance of the nutrient cycling functions (between 10–30% important OTUs) and restricted the functions that enhancing plant stress tolerance (limited to top 10% most important OTUs).

Given that surrounding soil dominates rhizosphere microbiota assembly with endosphere contributions, we next investigated the contributions of soil and endosphere microbiotas to re-assembled rhizosphere functions. Most of the rhizosphere bacterial taxa referring to stress tolerance functions (top 30% most important OTUs in black and paddy soils, top 10% most important OTUs in red soil) were in low relative abundance (RA < 1.81%) and bulk soil sourced (Fig. 4b), especially for the keystone OTUs (Fig. 4c and Additional file: Figure S5c). For nutrient cycling functions, most OTUs were also bulk soil sourced, but two black soil associated OTUs, Klebsiella and Pseudomonas (both belong to Gammaproteobacteria), were observed abundant in rhizosphere after transplanted to red soil (Fig. 4d).

Discussion

Plants exert strong selection on their root-associated microbiota and most members are initially recruited from surrounding soils [19]. The recruitment decreases the diversity of bacterial community from soil to rhizosphere and then to endosphere. Previous works demonstrate that the composition of soil bacterial communities are largely influenced by environmental variability [20, 21]. Therefore, in our research, the composition of rhizosphere and endosphere microbiotas were primarily dominated by soil type. However, we observed many rhizosphere Gammaproteobacterial groups were not soil dependent after transplanted from black soil to red soil. This may indicate that endosphere bacteria recruited from black soil were released and colonized in rhizosphere after transplanted to red soil. These results confirmed that rhizosphere microbiota succession was bidirectionally driven by both soil and endosphere communities. Therefore, there is a great need to increase understanding of how environmental conditions affect plant-microbe interactions [22].

Compared to the microbiota compositions, we observed less differed functional traits among different types of soil. This may suggest that soils dependent distinctive microbial taxa were less divergent in functional gene reservoir. When plants grow in unoccupied soil habitats, they recruit microorganisms to support their functional requirements although these microbial populations may belong to different taxa from distinct soil environments. Bell et al. [23] find the shifts in structure of rhizosphere microbiota strongly correlates with soil N availability and suggest that plants shift the structure and function of rhizosphere microbiota are likely to affect their competitive ability and fitness.

The functional profiles of rhizosphere microbiota showed different patterns among soils. The most important rhizosphere functions were help to enhance the ability of plant abiotic/biotic stress tolerance, including “Flavonoid biosynthesis”, “Streptomycin biosynthesis” and “Glycosphingolipid biosynthesis” [17, 18], followed by the functions related to nutrient cycling. However, the importance of nutrient cycling related functions were differed among soils due to different available nutrient concentrations. We observed the nutrient cycling related functions were marginalized in nutrient excessive soils while valued in nutrient deficient soils. Interestingly, two black soil associated OTUs (Klebsiella and Pseudomonas of Gammaproteobacteria) were observed abundant in rhizosphere after transplanted to red soil. Many plant-associated members of these two taxa are discovered to enhance nitrogen and phosphorus availability for plant [24, 25]. This dramatic colonization of endophytes in rhizosphere may reflect strong functional compensation under nutrient deficiency conditions in red soil. Consequently, it can be argued that the plant required functional rather than compositional characteristics appear to be a predictable principle that governing rhizosphere microbiota assembly.

Conclusions

Functional microbiotas are essential for agro-ecosystem productivity. Overall, we show that plants prefer to regulate rhizosphere microbiota to improve their fitness in different soil environments. When plants were grown in nutrient excessive soils (Fig. 5a), nutrient cycling functions in rhizosphere microbiota may be marginalized, while when grown in nutrient deficient soils (Fig. 5b), plants will sacrifice a proportion of stress tolerance functions and compensatory endophytes may colonize the rhizosphere to satisfy nutrient provisions. Taken together, our findings demonstrate that soil condition triggered functional compensation for host fitness requirement drive plant rhizosphere microbiota assembly.

Declarations

Ethics approval and consent to participate

Not applicable

Consent for publication

Not applicable

Availability of data and materials

The authors declare that the data supporting the findings of this study are available within the paper and its Supplementary Information files. All DNA sequences are deposited in National Center for Biotechnology Information under accession numbers PRJNA593913 and PRJNA594090.

The “vegan”, “ggplot2”, “psych” and “edgeR” are packages for the R statistical language and environment. The codes for vegan (https://cran.r-project.org/package=vegan), ggplot2 (https://cran.r-project.org/package=ggplot2), psych (https://cran.r-project.org/package=psych) and edgeR (http://www.bioconductor.org/packages/release/bioc/html/edgeR.html) are freely available on the web.

Competing interests

The authors declare no conflict of interest.

Funding

This research was supported by the Young Elite Scientists Sponsorship Program by CAST (2018QNRC001), the Agricultural Science and Technology Innovation Program of CAAS (CAAS-ZDRW202009), the Fundamental Research Funds for the Central Universities (KYXK202004 & KYT201802) and the Innovative Research Team Development Plan of the Ministry of Education of China (IRT_17R56).

Authors’ contributions

W.-B.X., R.Z., Q.S., and Y.R. designed the study, created the figures and wrote the manuscript. Y.R., H.Y., and A.M. performed experimental work, sampling and DNA sequencing. Y.R., W.-B.X., and W.X. carried out the bioinformatics and statistical analysis. All authors helped edit and complete the manuscript.

Acknowledgments

The authors thank the staff at the Yingtan Red Soil Ecological Experiment Station of Chinese Academy of Sciences for helping with the collection of soil samples.

References

1. Zhang J, Liu Y-X, Zhang N, Hu B, Jin T, Xu H, et al. NRT1.1B is associated with root microbiota composition and nitrogen use in field-grown rice. Nat Biotechnol. 2019;37:676–84.

2. Yang J, Kloepper JW, Ryu C-M. Rhizosphere bacteria help plants tolerate abiotic stress. Trends Plant Sci. 2009;14:1–4.
3. Kwak M-J, Kong HG, Choi K, Kwon S-K, Song JY, Lee J, et al. Rhizosphere microbiome structure alters to enable wilt resistance in tomato. Nat Biotechnol. 2018;36:1100–9.
4. Lundberg DS, Lebeis SL, Sur Herrera P, Scott Y, Jase G, Stephanie M, et al. Defining the core Arabidopsis thaliana root microbiome. Nature. 2012;488:86–90.
5. Castrillo G, Teixeira PJ, Paredes SH, Law TF, De LL, Feltcher ME, et al. Root microbiota drive direct integration of phosphate stress and immunity. Nature. 2017;543:513–8.
6. Zhalnina K, Louie KB, Hao Z, Mansoori N, Rocha UN da, Shi S, et al. Dynamic root exudate chemistry and microbial substrate preferences drive patterns in rhizosphere microbial community assembly. Nat Microbiol. 2018;3:470–80.
7. Bulgarelli D, Garrido-Oter R, Münch Philippc, Weiman A, Dröge J, Pan Y, et al. Structure and function of the bacterial root microbiota in wild and domesticated barley. Cell Host Microbe. 2015;17:392–403.
8. Edwards J, Johnson C, Santos-Medellín C, Lurie E, Podishetty NK, Bhatnagar S, et al. Structure, variation, and assembly of the root-associated microbiomes of rice. Proc Natl Acad Sci USA. 2015;112:E911–20.
9. Peiffer JA, Aymé S, Omry K, Zhao J, Susannah Green T, Dangl JL, et al. Diversity and heritability of the maize rhizosphere microbiome under field conditions. Proc Natl Acad Sci USA. 2013;110:6548–53.
10. Bulgarelli D, Schlaeppi K, Spaepen S, van Themaat EVL, Schulze-Lefert P. Structure and functions of the bacterial microbiota of plants. Annu Rev Plant Biol. 2013;64:807–38.
11. Berg G, Raaijmakers JM. Saving seed microbiomes. ISME J. 2018;12:1167–70.
12. Yan Y, Kuramae EE, de Hollander M, Klinkhamer PGL, van Veen JA. Functional traits dominate the diversity-related selection of bacterial communities in the rhizosphere. ISME J. 2017;11:56–66.
13. Walters WA, Jin Z, Youngblut N, Wallace JG, Sutter J, Zhang W, et al. Large-scale replicated field study of maize rhizosphere identifies heritable microbes. Proc Natl Acad Sci USA. 2018;115:7368–73.
14. Niu B, Paulson JN, Zheng X, Kolter R. Simplified and representative bacterial community of maize roots. Proc Natl Acad Sci USA. 2017;2450–9.
15. Hacquard S, Garrido-Oter R, González A, Spaepen S, Ackermann G, Lebeis S, et al. Microbiota and host nutrition across plant and animal kingdoms. Cell Host Microbe. 2015;17:603–16.
16. Langille MGI, Zaneveld J, Caporaso JG, McDonald D, Knights D, Reyes JA, et al. Predictive functional profiling of microbial communities using 16S rRNA marker gene sequences. Nat Biotechnol. 2013;31:814–21.
17. Winkel-Shirley B. Biosynthesis of flavonoids and effects of stress. Curr Opin Plant Biol. 2002;5:218–23.

18. Silva ACR da, Ferro JA, Reinach FC, Farah CS, Furlan LR, Quaggio RB, et al. Comparison of the genomes of two Xanthomonas pathogens with differing host specificities. Nature. 2002;417:459–63.
19. Tkacz A, Cheema J, Chandra G, Grant A, Poole PS. Stability and succession of the rhizosphere microbiota depends upon plant type and soil composition. ISME J. 2015;9:2349–59.
20. Xun W, Huang T, Zhao J, Ran W, Wang B, Shen Q, et al. Environmental conditions rather than microbial inoculum composition determine the bacterial composition, microbial biomass and enzymatic activity of reconstructed soil microbial communities. Soil Biol Biochem. 2015;90:10–8.
21. Noah F, Jackson RB. The diversity and biogeography of soil bacterial communities. Proc Natl Acad Sci USA. 2006;103:626–31.
22. Cheng Y, Zhang L, He S. Plant-microbe interactions facing environmental challenge. Cell Host Microbe. 2019;26:183–92.
23. Bell CW, Asao S, Calderon F, Wolk B, Wallenstein MD. Plant nitrogen uptake drives rhizosphere bacterial community assembly during plant growth. Soil Biol Biochem. 85:170–82.
24. Lidbury IDEA, Murphy ARJ, Scanlan DJ, Bending GD, Jones AME, Moore JD, et al. Comparative genomic, proteomic and exoproteomic analyses of three Pseudomonas strains reveals novel insights into the phosphorus scavenging capabilities of soil bacteria. Environ Microbiol. 2016;18:3535–49.
25. Elmerich C. Molecular biology and ecology of diazotrophs associated with non-leguminous plants. Nat Biotechnol. 1984;2:967–78.
26. Edgar RC. UPARSE: highly accurate OTU sequences from microbial amplicon reads. Nat Methods. 2013;10:996–8.
27. Price MN, Dehal PS, Arkin AP. Fasttree: computing large minimum evolution trees with profiles instead of a distance matrix. Mol Biol Evol. 2009;26:1641–50.
28. Smits SA, Leach J, Sonnenburg ED, Gonzalez CG, Lichtman JS, Reid G, et al. Seasonal cycling in the gut microbiome of the Hadza hunter-gatherers of Tanzania. Science. 2017;357:802–6.
29. Benjamini Y, Hochberg Y. Controlling the false discovery rate: a practical and powerful approach to multiple testing. J R Stat Soc B. 1995;57:289–300.
30. Bastian M, Heymann S, Jacomy M. Gephi: an open source software for exploring and manipulating networks. Proc 3rd Intl ICWSM Conf. 2009;361–2.
31. Marasco R, Mosqueira MJ, Fusi M, Ramond J-B, Merlino G, Booth JM, et al. Rhizosheath microbial community assembly of sympatric desert speargrasses is independent of the plant host. Microbiome. 2018;6:215.
32. Shannon P, Markiel A, Ozier O, Baliga NS, Wang JT, Ramage D, et al. Cytoscape: a software environment for integrated models of biomolecular interaction networks. Genome Res. 2003;13:2498–504.
33. Kanehisa M, Goto S. KEGG: kyoto encyclopedia of genes and genomes. Nucleic Acids Res. 2000;28:27–30.

Figures

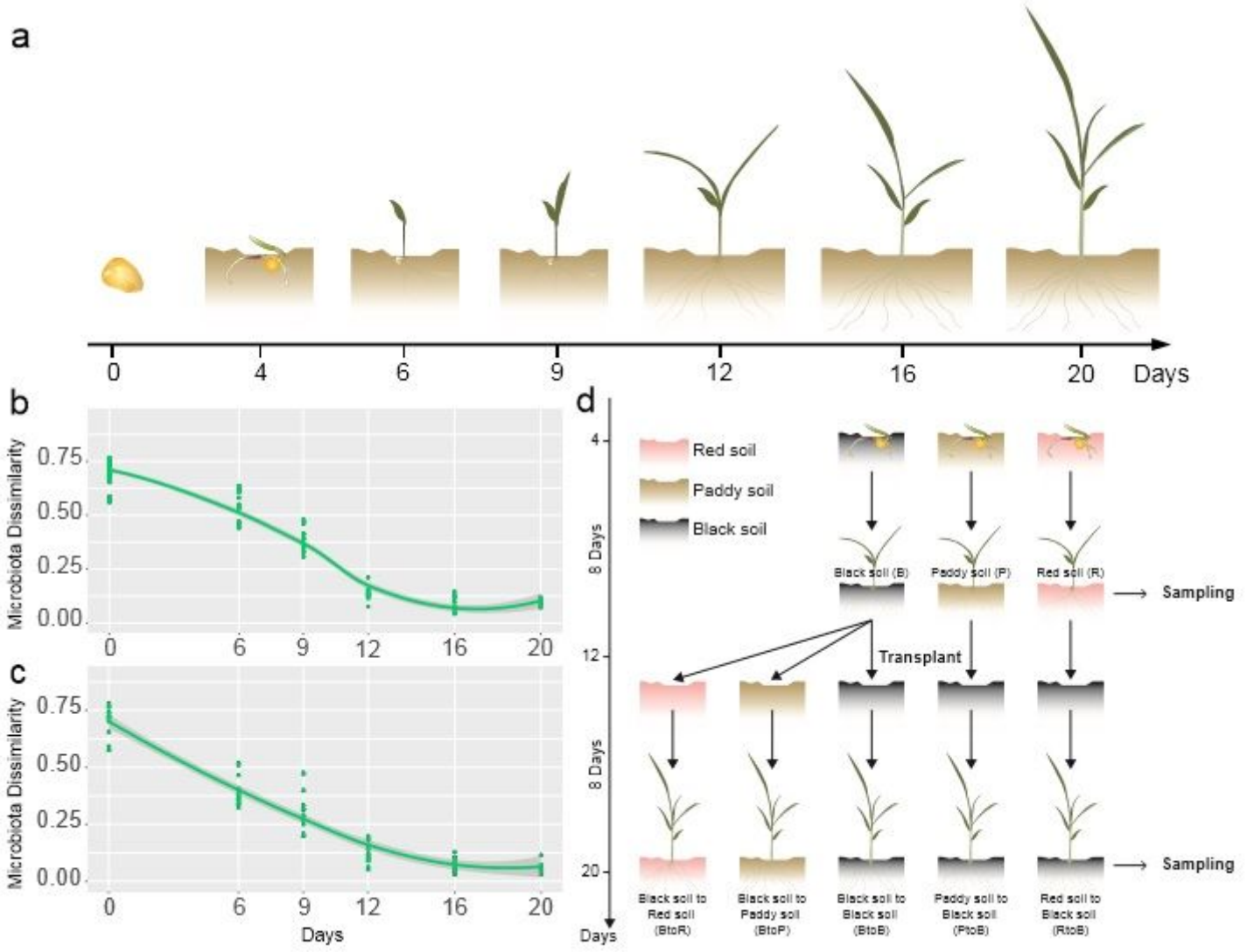

Figure 1

Diagram of experimental design. (a) Diagram of experimental design for root microbiota changes at successive intervals. (b) Weighted_UniFracmicrobiota dissimilarity between rhizospheremicrobiotas on each sampling time point and microbiota on day 20. The bulk soil microbiota is considered as rhizospheremicrobiota on day 0. (c)Weighted_UniFracmicrobiota dissimilarity between endospheremicrobiotas on each sampling time point and microbiota on day 20. The seed microbiota is considered as endospheremicrobiota on day 0. (d) Experimental design of transplanting experiment.

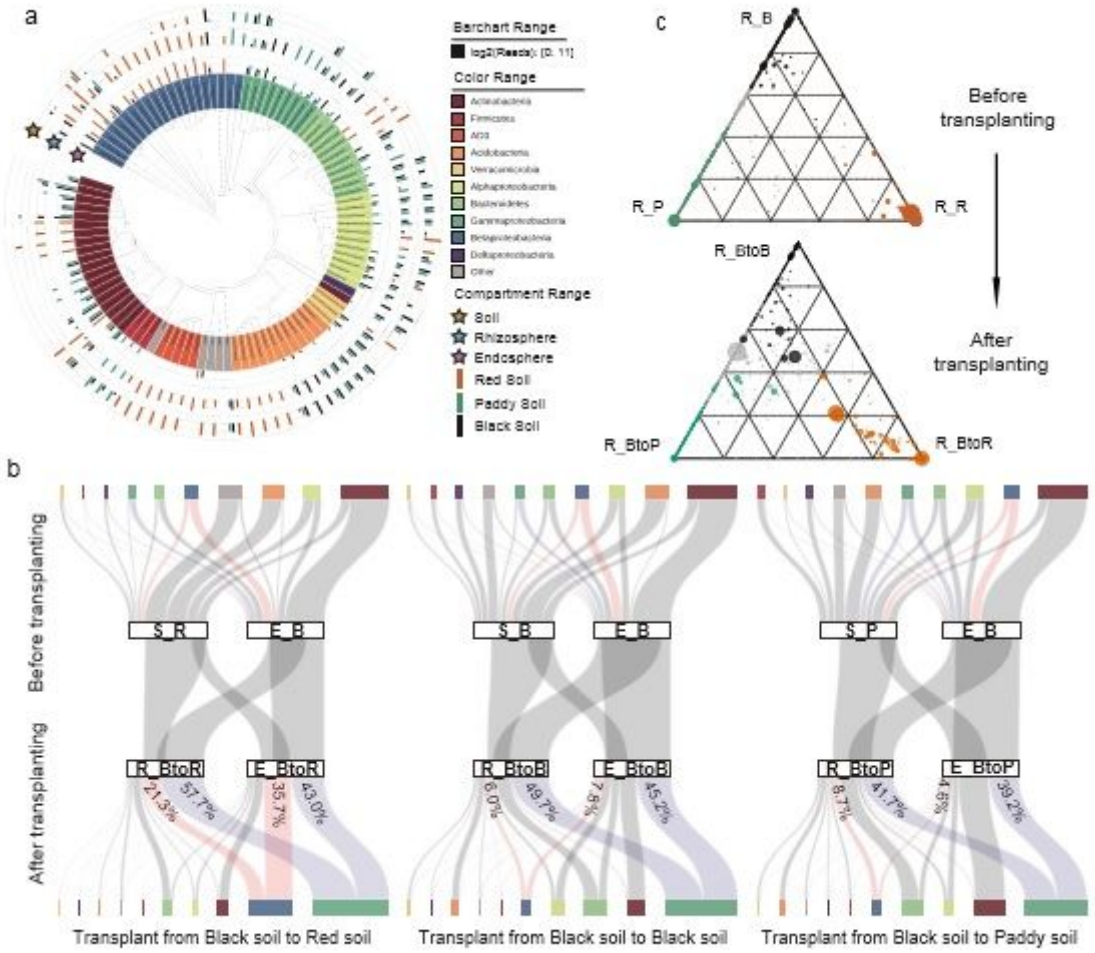

Figure 2

The taxonomical shifts of maize root microbiota in transplanting experiment. (a)Phylogenetic tree of the top 100 OTUs in different compartments in three types of soil before transplanting. Inner ring represents detected OTUs. Peripheral barchart represents relative abundances. (b)Sankey plots of bacterial taxonomic flow on phylum level during transplanting. Color bars indicate different bacterial phyla in (a). Pink and lavender color flows indicate variations of Betaproteobacteria and Gammaproteobacteria, respectively. (c)Ternary plots of all detected OTUs at rhizosphere microhabitats during transplanting. Each point represents one OUT. Point size represents relative abundance and position is determined by the contribution of three microbiotas to the total relative abundance. Black, Green and Orange points mark OTUs significantly enriched (FDR, P-value < 0.05) from black, paddy and red soil, respectively. Gray points indicate OTUs not significantly changed.

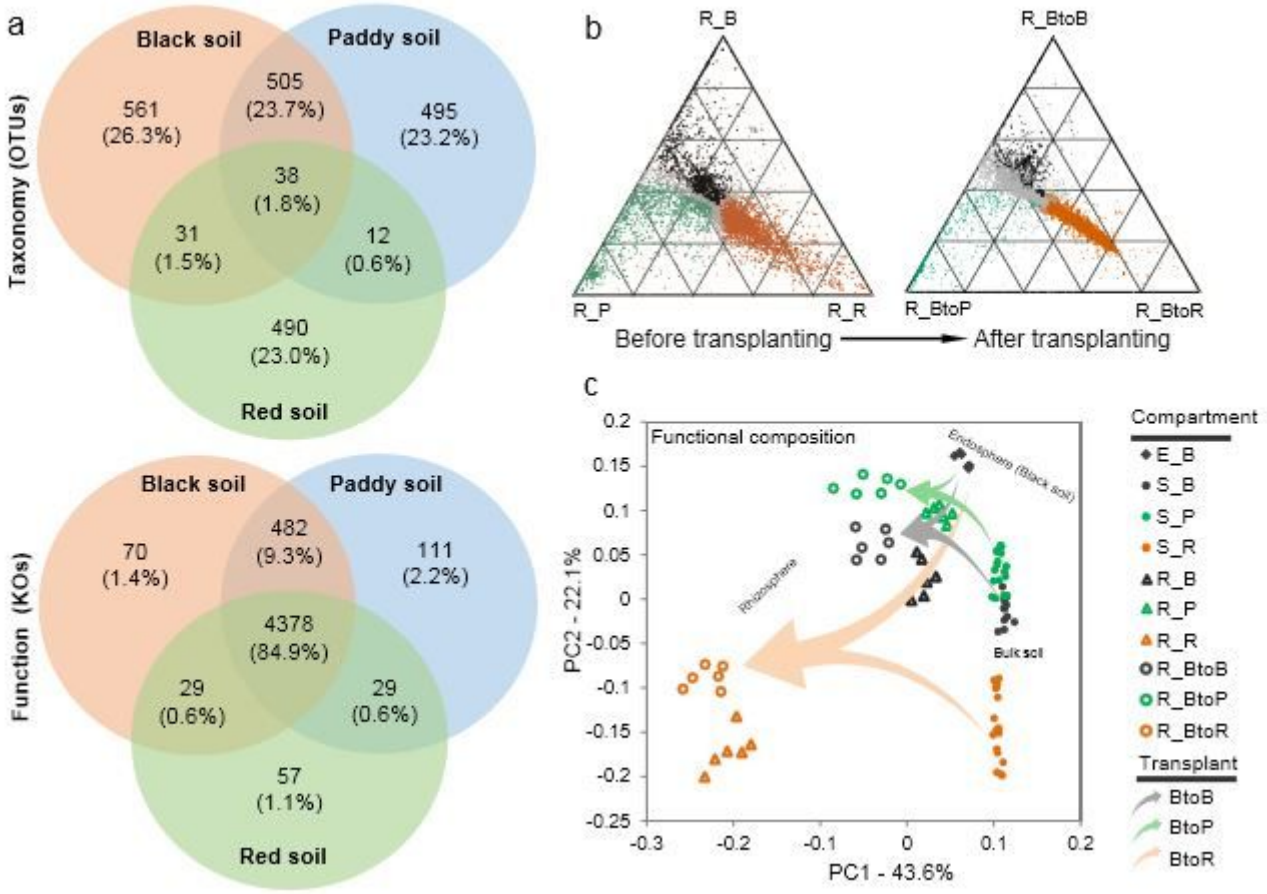

Figure 3

The shifts of rhizosphere functional profile in transplanting experiment. (a) The overlap of taxonomical OTUs (above) and functional KOs (below) in three types of bulk soil. (b) Ternary plots of all predicted KOs at rhizosphere microhabitats during transplanting. Each point represents one KO. Point size represents relative abundance and position is determined by the contribution of three microbiotas to the total relative abundance. Black, Green and Orange points mark KOs significantly enriched (FDR, P-value < 0.05) from black, paddy and red soil, respectively. Gray points indicate KOs not significantly changed. (c) Principal components analysis (PCA) of functional composition of microbiotas transplanting from black soil to three types of soil. S_B: Black soil. S_P: Paddy soil. S_R: Red soil. E_B: Endosphere in black soil before transplanting. R_BtoB: Rhizosphere after transplanted from black soil to black soil. R_BtoP: Rhizosphere after transplanted from black soil to paddy soil. R_BtoR: Rhizosphere after transplanted from black soil to red soil.

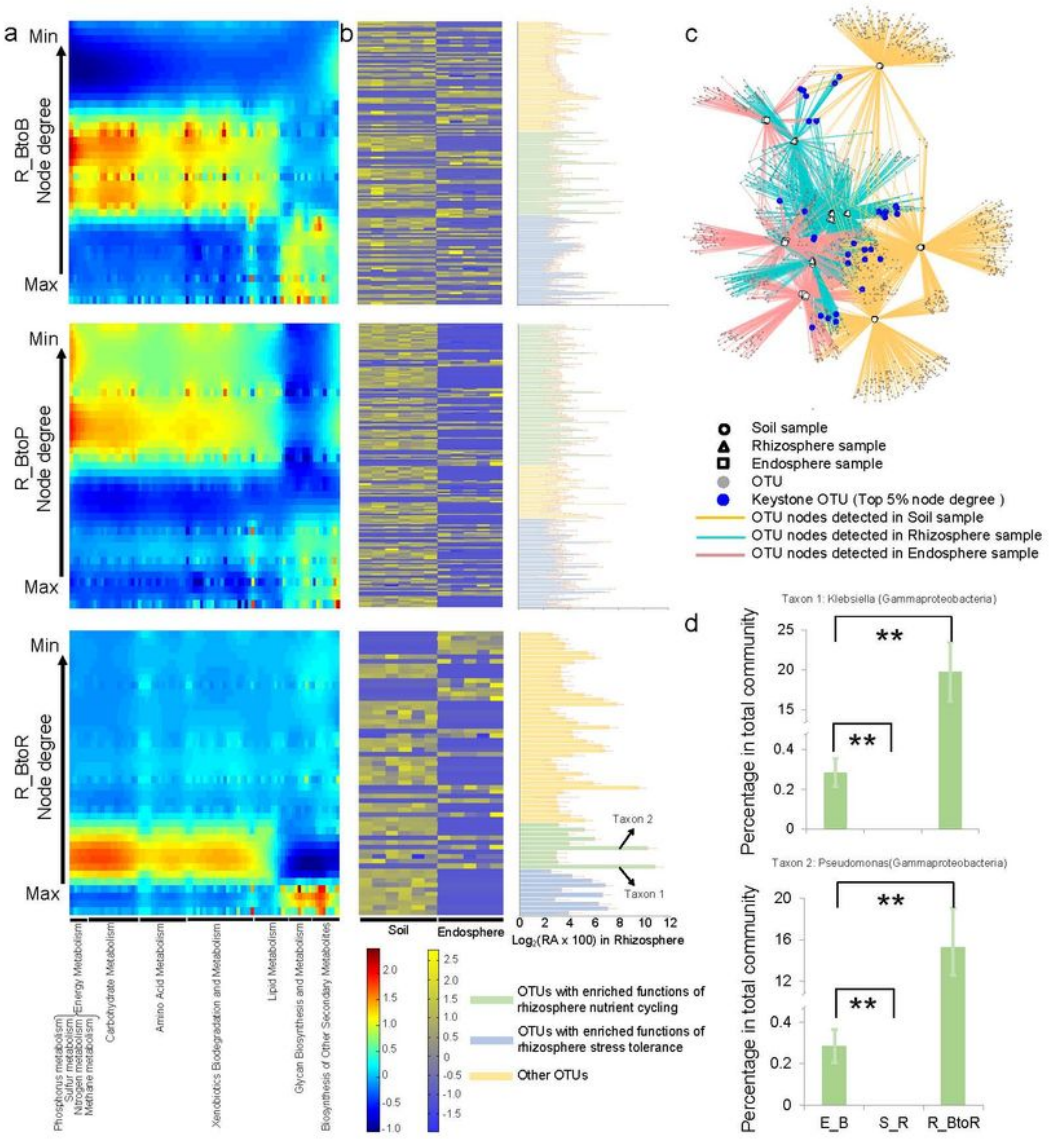

Figure 4

Functional and taxonomical characteristics of rhizospheremicrobiota after transplanting. (a) The rhizosphere functional profile distributed from highest importance to lowest. Color scale represents enrichment or reduction of predicted function comparing to theoretical function. (b) Heatmap of OTU sources from endosphere and bulk soil microbiotas and histogram of the relative abundance of OTU in re-assembled rhizospheremicrobiota. Color scale from greatest (yellow) to lowest (blue) taxonomical

contribution. All OTUs distributed along importance from highest to lowest corresponding to functional distribution in (a). Two abundant OTUs (taxon 1 and 2) are two specific endosphere sourced taxa contributed to nutrient cycling functions. (c) Bipartite network analysis of microbiotas after transplanting. Edges connecting samples (hollow circle, triangle and rectangle) to OTUs (gray point) were colored according to their compartments. The keystone OTUs were highlighted with green points. (d) The relative abundance of two OTU (taxon 1 and taxon 2 in (b)) in E_B, S_R and R_BtoR. Asterisks indicate significance: **P-value < 0.01.

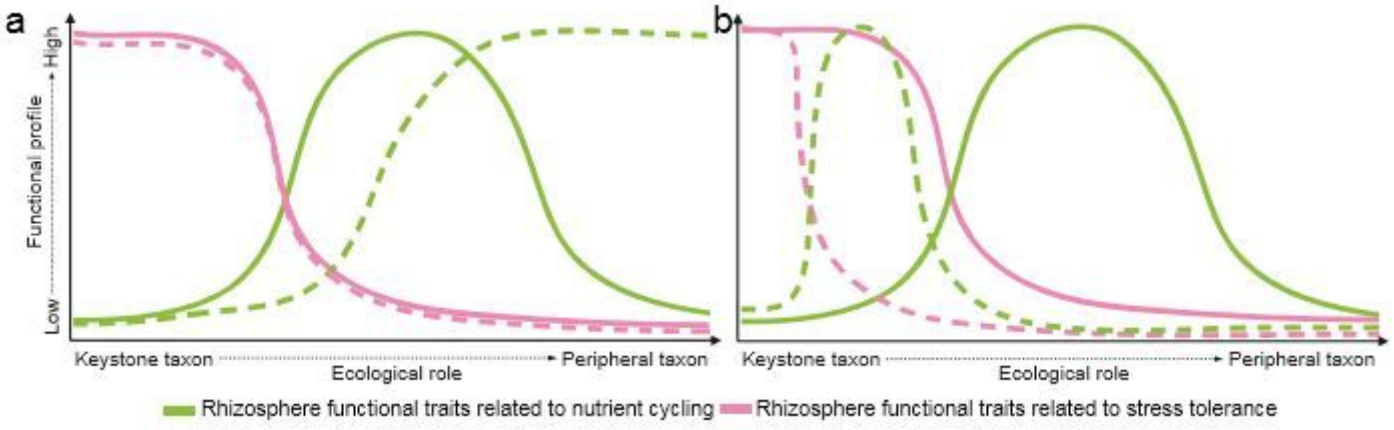

Figure 5

Conceptual model of functional assembly pattern in rhizospheremicrobiota under different soil conditions. (a) Plant rhizospheremicrobiota assembled in nutrient excessive soil. The nutrient cycling related functions in rhizospheremicrobiota may be marginalized. (b) Plant rhizospheremicrobiota assembled in nutrient deficient soil. A proportion of stress tolerance related functions may sacrifice to provide nutrient cycling related functions. Red line indicates the rhizosphere functional traits related to nutrient cycling and metabolism. Green line indicates the rhizosphere functional traits related to stress tolerance. Solid line represents an idealized functional distribution pattern. Dotted line represents practical functional distribution pattern under different soil condition.

Supplementary Files

This is a list of supplementary files associated with this preprint. Click to download.

- TableS3.pdf
- TableS4.pdf
- TableS5.pdf
- TableS2.pdf
- TableS1.pdf
- FigureS2.pdf
- FigureS5.pdf

- FigureS2.pdf
- FigureS3.pdf
- TableS1.pdf
- FigureS1.pdf
- FigureS1.pdf
- FigureS4.pdf
- TableS3.pdf
- TableS4.pdf
- TableS2.pdf
- FigureS5.pdf
- FigureS4.pdf
- FigureS3.pdf
- TableS5.pdf